Stem Cell Reports, Volume *11*

Supplemental Information

Cell Surface N-Glycans Influence Electrophysiological Properties and Fate Potential of Neural Stem Cells

Andrew R. Yale, Jamison L. Nourse, Kayla R. Lee, Syed N. Ahmed, Janahan Arulmoli, Alan Y.L. Jiang, Lisa P. McDonnell, Giovanni A. Botten, Abraham P. Lee, Edwin S. Monuki, Michael Demetriou, and Lisa A. Flanagan

Supplemental Figures

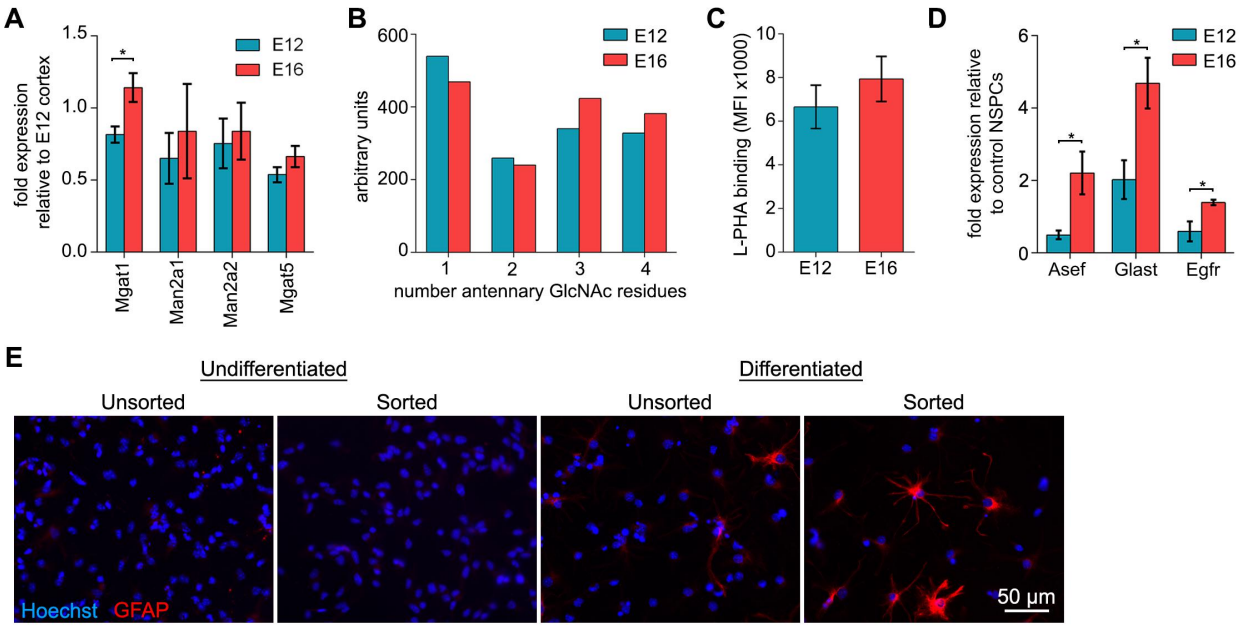

Figure S1. Analysis of E12, E16, and sorted astrocyte-biased NSPCs. Related to Figures 1 and 2. (A) Analysis of N-glycan branching enzyme gene expression by qRT-PCR indicates higher levels of expression in E16 compared to E12 NSPCs (*Mgat1*, p=0.015, unpaired Student's t-test). Values for E12 and E16 NSPCs are relative to E12 cortex (see Supplemental Experimental Procedures). (B) Plasma membrane N-glycans of E12 and E16 NSPCs analyzed by MALDI-TOF mass spectrometry reveal differences in numbers of GlcNAc residues attached to the trimannosyl core (referred to here as branches). One branch corresponds to mono-antennary GlcNAc structures and 2 branches to bi-antennary structures. Three branches correspond to either tri-antennary structures or bi-antennary sugars also containing a bisected GlcNAc. Four branches correspond to either tetra-antennary structures or tri-antennary sugars also containing a bisected GlcNAc. E12 NSPCs contain more 1 or 2 branched N-glycans while E16 NSPCs have more with 3 or 4 branches (n=1). (C) Flow cytometry analysis with lectin L-PHA to detect cell surface highly branched N-glycans indicates similar levels of these structures on E12 and E16 NSPCs, with a trend toward higher levels on E16 cells. Data is represented as mean fluorescence intensity (MFI). (D) Analysis of astrocyte progenitor marker expression by qRT-PCR indicates higher levels of expression in E16 compared to E12 NSPCs (*Asef*, p=0.0300; *Glast*, p=0.0234; *Egfr*, p=0.0311; unpaired Student's t-test). Values for E12 and E16 NSPCs are relative to an independent E12 NSPC sample. (E) Unsorted and DEP-sorted E12 NSPCs were immunostained for GFAP. No GFAP expression was observed in undifferentiated unsorted controls or sorted cells. More GFAP-positive cells were observed in the differentiated sorted sample compared to control NSPCs. Images of differentiated GFAP-labeled cells are identical to those in Figure 2E. All error bars represent standard error of the mean. N=3 or more independent biological repeats unless otherwise noted, (*p<0.05).

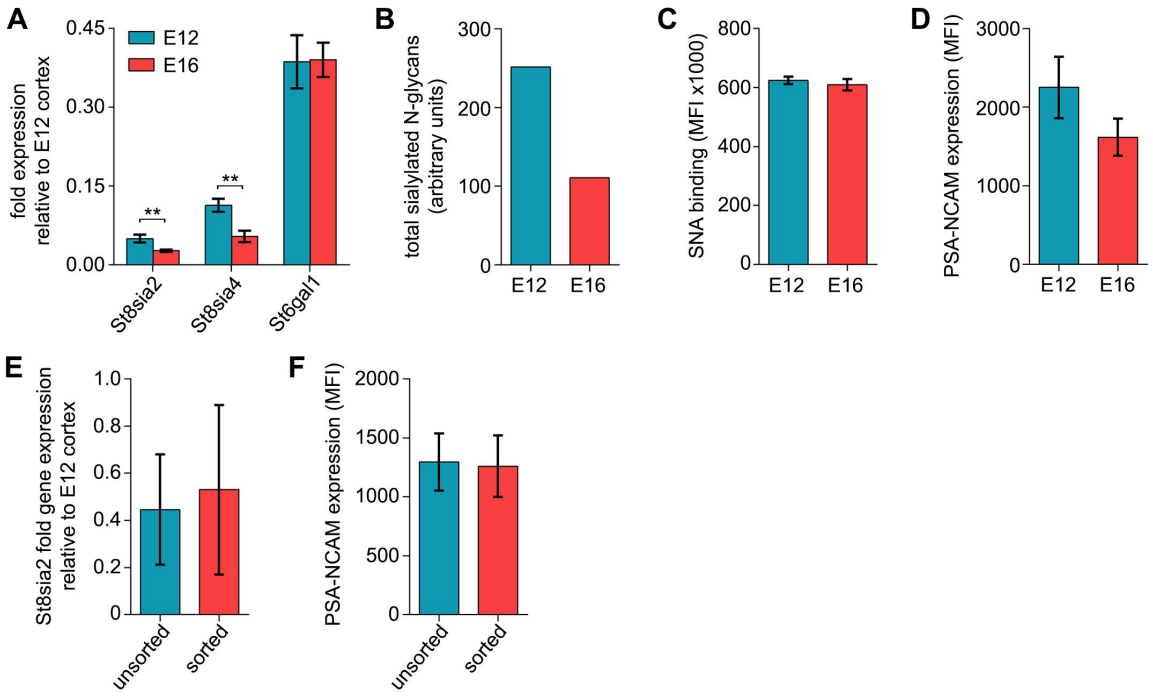

Figure S2. Characterization of NSPC sialic acid. Related to Figures 1 and 2. (A) qRT-PCR gene expression analysis of transcripts encoding sialic acid modifying enzymes indicates higher expression of *St8sia2* and *St8sia4* in E12 compared to E16 NSPCs (*St8sia2*, p=0.007, *St8sia4*, p=0.0072, unpaired Student's t-test). There was no difference in *St6gal1* expression between the two cell populations. Values for E12 and E16 NSPCs are relative to those of E12 cortex. (B) Analysis of plasma membrane N-glycans from E12 and E16 NSPCs by MALDI-TOF mass spectrometry shows more sialic acid modified N-glycans on E12 than E16 NSPCs (n=1). (C) Flow cytometry analysis with lectin SNA to detect cell surface sialic acid containing N-glycans modified by ST6GAL1 indicates similar levels of these structures on E12 and E16 NSPCs. Data is represented as mean fluorescence intensity (MFI). (D) Flow cytometry analysis of PSA-NCAM indicates a non-significant lower (p=0.0891) expression of PSA-NCAM on E16 NSPCs compared to E12 NSPCs. Data represented as MFI. (E) Expression of the sialic acid modifying enzyme *St8sia2* analyzed by qRT-PCR indicates similar levels in control and sorted astrocyte-biased NSPCs. Values for E12 NSPCs and sorted cells are relative to those of E12 cortex. (F) Flow cytometry analysis of PSA-NCAM indicates similar levels between control and sorted cells. All error bars represent standard error of the mean. N=3 or more independent biological repeats unless otherwise noted, (**p<0.01).

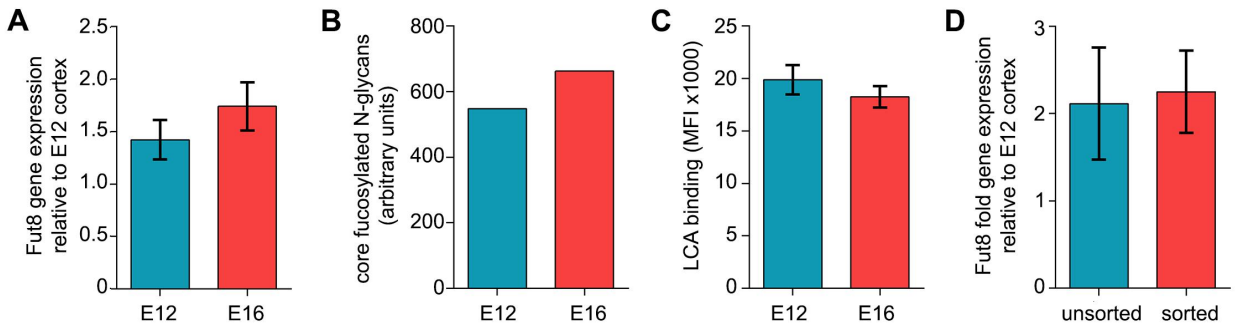

Figure S3. Characterization of NSPC core fucose glycosylation. Related to Figures 1 and 2. (A) qRT-PCR gene expression analysis of transcripts encoding the *Fut8* enzyme that adds core fucose indicates similar levels in E12 and E16 NSPCs. Values for E12 and E16 NSPCs are relative to those of E12 cortex. (B) Plasma membrane N-glycans of E12 and E16 NSPCs analyzed by MALDI-TOF mass spectrometry show similar amounts of core fucose modified N-glycans on E12 and E16 NSPCs (n=1). (C) Flow cytometry analysis with lectin LCA to detect cell surface core fucose containing N-glycans indicates similar levels of these structures on E12 and E16 NSPCs. Data is represented as mean fluorescence intensity (MFI). (D) Expression of *Fut8* analyzed by qRT-PCR indicates similar levels in control and sorted E12 NSPCs. Values for E12 NSPCs and sorted cells are relative to those of E12 cortex. All error bars represent standard error of the mean. N=3 or more independent biological repeats unless otherwise noted.

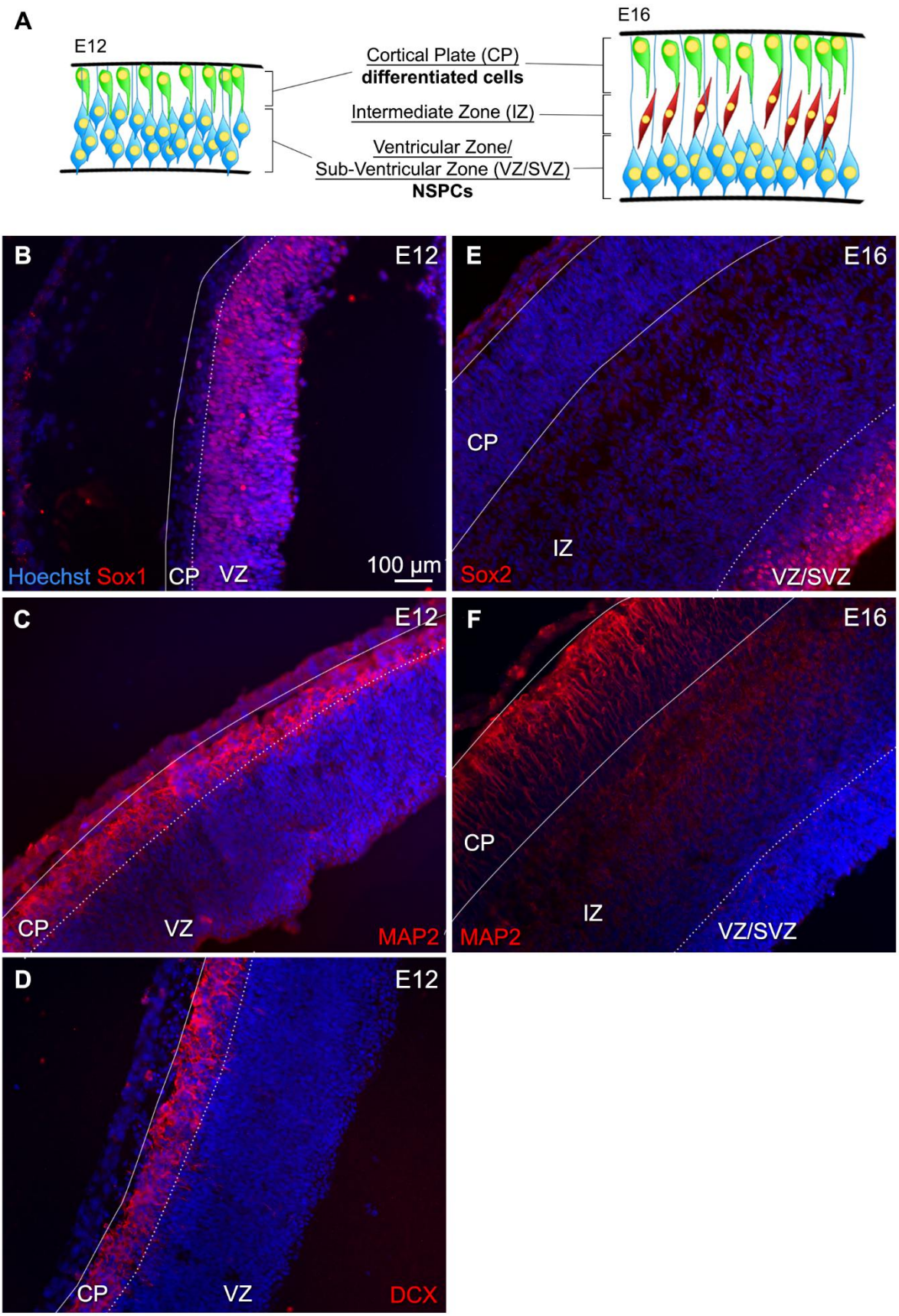
A
E12
E16
Cortical Plate (CP)
differentiated cells
Intermediate Zone (IZ)
Ventricular Zone/
Sub-Ventricular Zone (VZ/SVZ)
NSPCs
B
E12
Hoechst Sox1
CP
VZ
100 µm
E
E16
CP
IZ
Sox2
VZ/SVZ
C
E12
CP
VZ
MAP2
F
E16
CP
IZ
MAP2
VZ/SVZ
D
E12
CP
VZ
DCX

Figure S4. Identification of the VZ/SVZ and CP during embryonic cortical development. Related to Figure 3. **(**A) Schematic representing the layers of the developing cerebral cortex depicts the VZ and CP at E12 and the VZ/SVZ, IZ, and CP at E16. Stem and progenitor cells in the VZ/SVZ are shown in blue, migrating cells in the IZ are in red, and the differentiated cells of the CP are in green. (B) Sagittal sections of the E12 mouse embryonic cortex were stained with antibodies to SOX1 to identify NSPCs and define the borders of the VZ. (C) E12 sagittal sections stained with antibodies to MAP2 to identify differentiated neurons define the borders of the CP. (D) Similarly, DCX antibodies detect differentiated neurons in the E12 CP. (E) Sagittal sections of the E16 mouse embryonic cortex were stained with antibodies to SOX2 to mark the NSPCs of the VZ/SVZ. (F) MAP2 staining of E16 sagittal sections marks the differentiated neurons in the CP; note the intervening IZ between the VZ/SVZ and CP at E16. All cell nuclei were labeled with Hoechst.

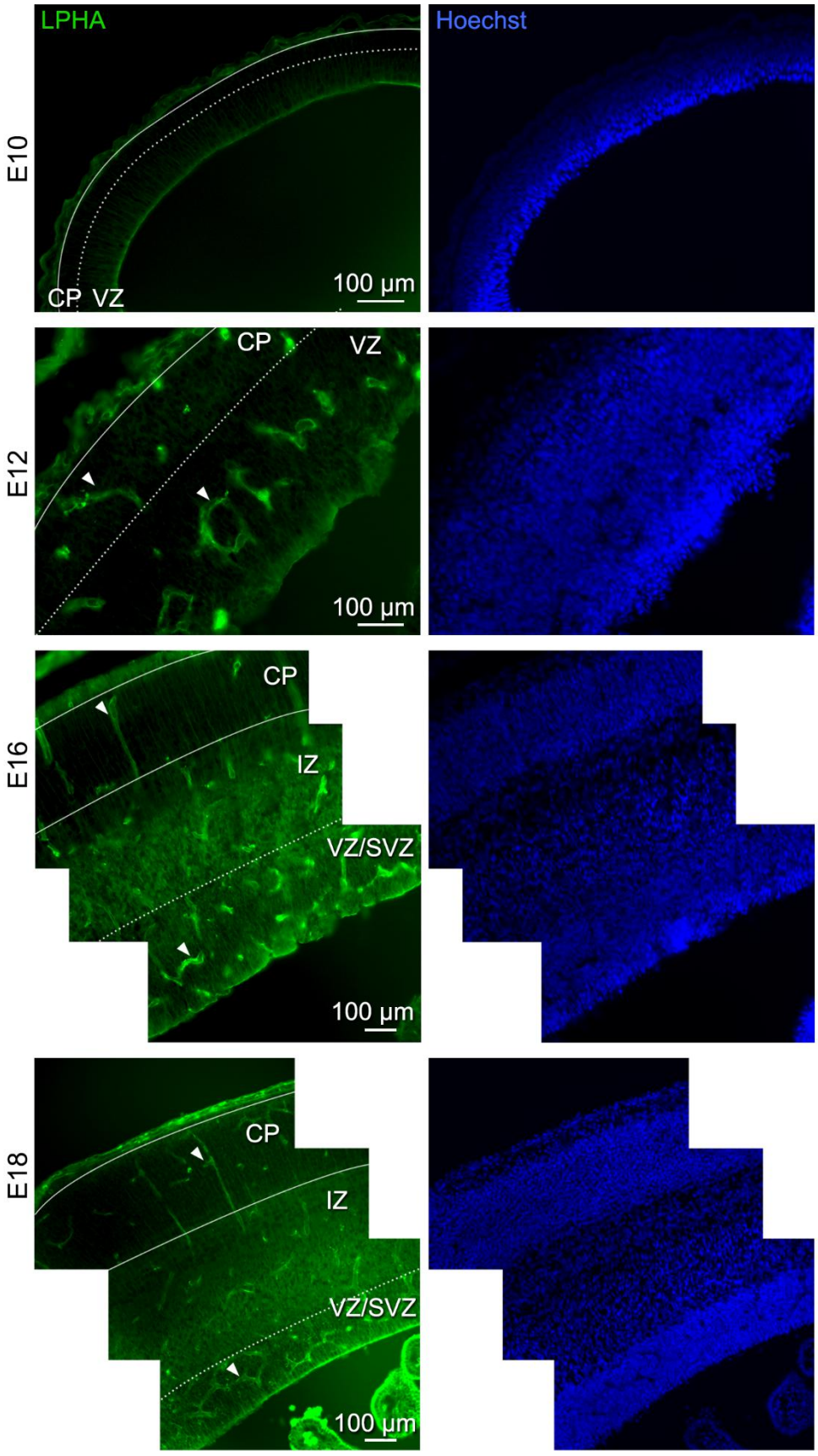
LPHA
Hoechst
E10
CP
VZ
100 μm
E12
CP
VZ
100 μm
E16
CP
IZ
VZ/SVZ
100 μm
E18
CP
IZ
VZ/SVZ
100 μm

Figure S5. Labeling of the E10 to E18 developing cerebral cortex with lectin L-PHA to detect highly branched N-glycans. Related to Figure 3. Lectin L-PHA indicates the presence of highly branched tetra-antennary N-glycans in sagittal sections of the developing embryonic cerebral cortex at E10, E12, E16, and E18. Dotted lines denote the boundaries between the NSPC niches (VZ in E12 and VZ/SVZ in E16) and regions containing more differentiated cells, the cortical plate (CP) and migrating progenitors, intermediate zone (IZ). Solid lines indicate the outer boundaries of the CP and IZ. Arrowheads point to blood vessels, which stain strongly for L-PHA and were excluded from quantitative analysis. More intense L-PHA staining is evident in the E16 and E18 NSPC niche (VZ/SVZ) than the E10 or E12 niche (VZ). Right hand panels are corresponding Hoechst stained nuclei for each panel on the left. Images of E12 and E16 LPHA-stained sections are identical to those in Figure 3A.

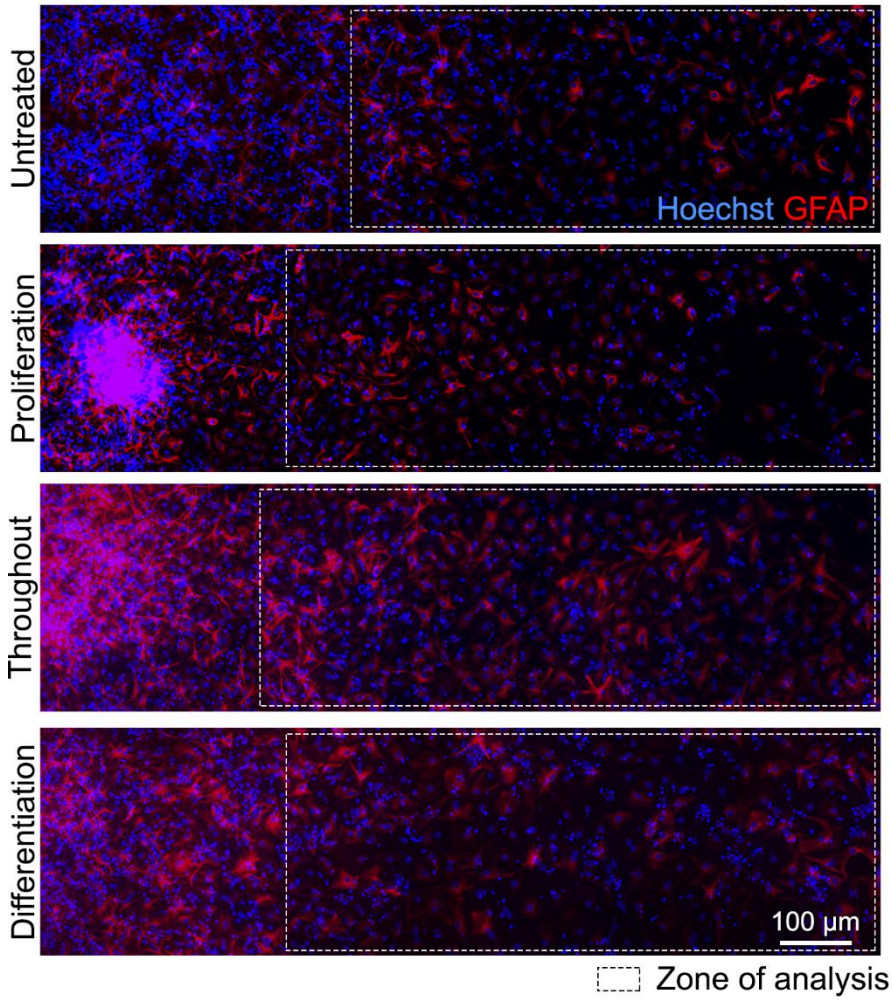

Figure S6. Whole field images of GFAP-positive cells. Related to Figure 6. Images of GFAP-positive astrocytes differentiated from E12 NSPCs indicate the zones of cells used for analysis (dashed boxes) to avoid high cell density regions (left side of each image). Cells were untreated or treated with 80 mM GlcNAc during proliferation, throughout proliferation and differentiation, or during differentiation (see Figure 6A). All cell nuclei were labeled with Hoechst.

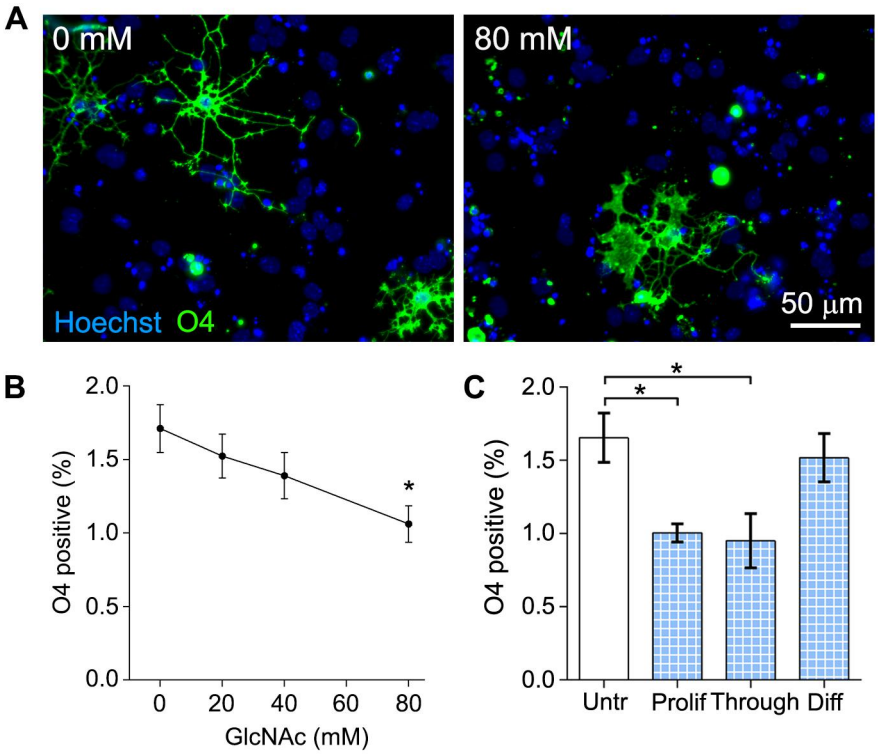

Figure S7. GlcNAc treatment decreases oligodendrocyte formation from E12 mouse NSPCs. Related to Figure 6. (A) E12 NSPCs treated with 80 mM GlcNAc during 3 days as undifferentiated cells and for an additional 7 days during differentiation generated fewer oligodendrocytes stained with O4 (green) than control NSPCs (0 mM, untreated). Some non-specific globular signal was present in all samples and was excluded from analysis. All nuclei were labeled with Hoechst (blue). (B) The percentage of O4-positive oligodendrocytes formed from E12 NSPCs decreases with increasing GlcNAc concentration (one-way ANOVA, p=0.0222). *Post hoc* analysis by Dunnett's test indicates significant decrease in oligodendrocyte formation after supplementation with 80 mM GlcNAc (p=0.0161) compared to untreated E12 NSPCs. (C) E12 NSPCs were treated with 80 mM GlcNAc in the proliferation stage (Prolif, 3 days), throughout both proliferation and differentiation stages (Through, 10 days), or during the differentiation stage (Diff, 7 days). The percentage of O4 positive oligodendrocytes was significantly decreased when NSPCs were treated with GlcNAc during the proliferation stage or throughout both stages (Untr v Prolif p=0.0383, Untr v Through p=0.0144, one-way ANOVA, Tukey *post hoc* for multiple comparisons) but not the differentiation stage, suggesting an effect on undifferentiated NSPCs but not differentiated cells. All error bars represent standard error of the mean. N=3 or more independent biological repeats, (*p<0.05).

Supplemental Tables

Table S1: **N-glycosylation enzymes of E12 and E16 NSPCs. Related to Figure 1**. Bolded enzymes show expression difference greater than 1.2-fold.

Enzyme	E16 fold over E12	Function
Man2a2	**1.6935**	**Removes mannose from N-glycans to initiate complex branching**
Fut8	**1.5476**	**Adds α1-6 linked fucose to first GlcNAc on N-glycan core**
B3gnt2	**1.5476**	**Involved in the formation of poly-N-acetyllactosamine**
St6gal1	**1.5263**	**Adds α2-6 linked sialic acid to galactose residues**
Man2a1	**1.2924**	**Removes mannose from N-glycans to initiate complex branching**
B4galt5	**1.2483**	**Adds galactose to N-glycans**
Mgat5	**1.2142**	**Adds β1-6 linked GlcNAc on highly-branched N-gycans**
Prkcsh	1.1810	B-subunit of glucosidase II
Mgat1	1.1567	Adds first β1-2 linked GlcNAc to form hybrid and complex N-glycans
Ganab	1.1408	A-subunit of glucosidase II; cleaves glucose from immature N-glycans in the ER
B4galt1	1.0000	Adds galactose to GlcNAc residues on branched N-glycans
St3gal2	1.0000	Adds α2-3 linked sialic acid to galactose
B3gnt4	0.9931	Biosynthesis of poly-N-acetyllactosamine
Mgat2	0.9794	Adds second β1-2 linked GlcNAc to form di-antennary N-glycans
Man1b1	0.9659	Removes mannose from N-glycans
B4galt3	0.9461	Adds first galactose for poly-N-acetyllactosamine chains
Man1a2	0.9395	Removes mannose from N-glycans necessary to initiate biosynthesis of branched N-glycans
Mogs	0.9013	Cleaves glucose from mannose in early N-glycan processing
Mgat4b	0.8888	Adds β1-4 linked GlcNAc on highly-branched N-gycans
Mgat4a	0.8526	Adds β1-4 linked GlcNAc on highly-branched N-gycans
Man1c1	0.8011	Removes mannose from N-glycans
Fut11	**0.7792**	**α1-3 fucosyltransferase**
B4galt2	**0.7423**	**Involved in the formation of poly-N-acetyllactosamine**
St8sia4	**0.5664**	**Also known as PST, biosynthesis of polysialic acid**
Mgat3	**0.5471**	**Adds β1-4 linked GlcNAc to form bisected N-glycans**
St8sia2	**0.2755**	**Also known as STX, biosynthesis of polysialic acid**
B3gnt8	low expr	Elongates branched N-glycans, strong activity toward tetra-antennary N-glycans
Man1a	low expr	Removes mannose from N-glycans necessary to initiate biosynthesis of branched N-glycans
Mgat4c	low expr	Adds β1-4 linked GlcNAc on highly-branched N-gycans
St8sia3	low expr	Biosynthesis of polysialic acid
B3gnt3	not expr	Involved in the formation of poly-N-acetyllactosamine
Man2b1	not expr	Removes mannose from N-glycans

Table S2: O-glycosylation enzymes of E12 and E16 NSPCs. Related to Figure 1. Bolded enzymes show expression difference greater than 1.2-fold.

Enzyme	E16 fold over E12	Function or possible function based on homology
Galnt7	**1.74**	**Adds galactose to pre-existing O-linked GalNAc on serine/threonine (S/T) residues**
Galnt4	**1.65**	**Adds initial GalNAc onto S/T in mucin-type O-glycans**
Pofut2	**1.37**	**Generates O-fucosylated proteins**
Pomt1	**1.23**	**Works with Pomt2 to generate O-mannose glycans**
Ogt	1.19	Adds initial GlcNAc to S/T to generate cytoplasmic and nuclear O-GlcNAc glycans
B3glct	1.1567	Transfers glucose to O-linked fucosyl glycans
Pomgnt1	1.07	Adds GlcNAc onto O-mannose glycans
Galnt1	1.06	Adds initial GalNAc onto S/T for mucin type O-glycans
St6GalNAc1	1.0479	Adds sialic acid to galactose residues of O-linked sugars
Pomt2	1	Works with Pomt1 to generate O-mannose glycans
Galnt11	0.97	Initiates biosynthesis of O-linked GalNAc glycans
Galnt2	0.97	Initiates biosynthesis of O-linked GalNAc glycans
C1galt1c1	0.97	Chaperone necessary for C1galt1 and core 1 O-glycan synthesis
C1galt1	0.93	Generates the core 1 O-glycan structure
Galnt10	0.87	Adds initial GalNAc onto S/T for mucin type O-glycans
Pofut1	0.85	Adds initial fucose to S/T to generate O-fucosylated proteins
Wbscr17	0.84	Initiates biosynthesis of O-linked GalNAc glycans
Galnt16	0.81	Adds initial GalNAc onto S/T in mucin-type O-glycans
St3gal1	**0.79**	**Adds sialic acid to galactose residues of O-linked sugars**
Galnt13	**0.68**	**Adds initial GalNAc onto S/T in mucin-type O-glycans**
Mgat5b	**0.48**	**Adds GlcNAc to mannose to generate branched O-mannose glycans**
Galnt12	low expr	Initiates biosynthesis of O-linked GalNAc glycans
Galnt14	low expr	Adds initial GalNAc onto S/T in mucin-type O-glycans
Galnt3	low expr	Adds initial GalNAc onto S/T in mucin-type O-glycans
Galnt9	low expr	Adds initial GalNAc on S/T in mucin-type O-glycans
Gcnt1	low expr	Generates the core 2 O-glycan structure
St8sia6	low expr	Biosynthesis of polysialic acid on O-glycans
A4gnt	low expr	Transfers GlcNAc to core 2 O-glycans to form type III mucins
Galnt5	not expr	Adds initial GalNAc onto S/T in mucin-type O-glycans
Galnt6	not expr	Adds initial GalNAc onto S/T in mucin-type O-glycans
Galntl5	not expr	Adds initial GalNAc onto S/T in mucin-type O-glycans
Galntl6	not expr	Adds initial GalNAc onto S/T in mucin-type O-glycans
Gcnt3	not expr	Involved in biosynthesis of core 2 and core 4 O-glycans of mucins

Table S3: Enzymes of E12 and E16 NSPCs involved in endoplasmic reticulum (ER) quality control, targeting of enzymes to lysosomes, or lysosomal degradation of glycans. Related to Figure 1. Bolded enzymes show expression difference greater than 1.2-fold.

Enzyme	E16 fold over E12	Function
Manba	**1.8921**	**Lysosomal mannosidase**
Hexa	**1.7901**	**A-subunit of lysosomal enzyme that degrades GM2 ganglioside**
Aga	**1.7532**	**Lysosomal enzyme; cleaves GlcNAc-Asn linkage on N-linked glycoproteins**
Fuca1	**1.2924**	**Lysosomal enzyme; degrades fucose containing glycoproteins**
Nagpa	**1.2746**	**Cleaves GlcNAc from mannose; involved in lysosomal enzyme trafficking from Golgi to lysosome**
Uggt1	**1.2142**	**Re-glucosylates N-glycans of misfolded proteins in the ER**
Edem3	1.1567	Participates in ER-associated degradation (ERAD) by cleaving mannose residues from N-glycans
Edem1	1.1408	Participates in ERAD by cleaving mannose residues from N-glycans and targets misfolded glycoproteins for degradation
Uggt2	1.0718	Re-glucosylates N-glycans of misfolded proteins in the ER
Hexb	1.0497	B-subunit of lysosomal enzyme that degrades GM2 ganglioside
Glb1	1.014	Lysosomal enzyme; involved in degradation
Neu3	1.0070	Plasma membrane sialidase
Neu1	0.9862	Lysosomal sialidase
Edem2	0.9461	Participates in ERAD by trimming mannose in the ER
Fuca2	0.9138	Lysosomal enzyme, degrades fucose containing glycoproteins
Gnptg	0.9075	Generates glycans necessary for trafficking lysosomal enzymes to lysosome
Gnptab	0.895	Generates glycans necessary for trafficking lysosomal enzymes to lysosome
Neu4	low expr	Lysosomal sialidase
Neu2	not expr	Cytoplasmic sialidase

Table S4: DNA primers for qRT-PCR. Related to Figure 2 and Supplemental Figure S1.

Gene	Forward Primer (5'→ 3')	Reverse Primer (5' → 3')	Expected length (bp)
Asef (probe 1)	TCTCCAGAGTCTCCGCATCTTC	GTGGCATCCATCACTTCGATG	353
Asef (probe 2)	GAGGAGGTGGAGAGCAACTG	GCGGTAGATGTCCTCGATGTTC	484
Slc1a3 (GLAST)	TTTCTCTCTAGGGGCAGGCT	CAGAAGGGAGGGCCTCTAGT	140
Egfr	TCTTCAAGGATGTGAAGTGTG	TGTACGCTTTCGAACAATGT	145
GAPDH	ATACGGCTACAGCAACAGGG	GCCTCTCTTGCTCAGTGTCC	105

Supplemental Experimental Procedures

NSPC cell culture:

CD-1 mice (Charles River) were purchased, selected randomly, and bred as approved by the University of California, Irvine Institutional Animal Care and Use Committee. Dorsal forebrain cortical tissue was dissected from the cerebral cortices of embryonic day 12.5 (E12) and 16.5 (E16) mice and placed in dissection buffer: PBS, 0.6% glucose, 50 U/mL Pen/Strep. Cortical tissue from multiple embryos within the same litter was pooled, and a subsequent culture from a single litter was considered a biological repeat. The tissue was dissociated using 0.05% Trypsin-EDTA at 37^{o}C for 10 min. Afterward, trypsin was inhibited using soybean trypsin inhibitor (Life Technologies) and dissociated cells were re-suspended in proliferation medium containing DMEM, 1x B27, 1x N2, 1 mM sodium pyruvate, 2 mM L-glutamine, 1 mM N-acetylcysteine, 20 ng/mL EGF, 10 ng/mL bFGF, and 2 µg/mL heparin. Cells were seeded at 150,000 cells/mL into non-tissue culture treated plastic plates and grown as non-adherent spheres. Cell cultures were passaged approximately every 3 days using enzyme-free NeuroCult Chemical Dissociation Kit (Mouse) (StemCell Technologies). All NSPC cultures were passaged at least once prior to experimental use. NSPCs were plated as adherent cultures for differentiation. HCl-washed German glass coverslips (Assistant/Carolina Biological Supply, Burlington, NC) were pretreated with poly-D-lysine (40 µg/mL in milliQ H_20) for 5 minutes then coated with laminin (20 µg/mL in EMEM) at 37^{o}C for 24 hours prior to cell adhesion. Whole neurospheres were seeded onto the laminin-coated coverslips in proliferation medium. After 24 hours, proliferation medium was removed and replaced with differentiation medium (same components as proliferation medium but excluding EGF, bFGF, and heparin) to induce differentiation. NSPCs were differentiated into neurons and astrocytes in these conditions for 3 days and oligodendrocytes for 7 days. For 7 day differentiated samples, culture media was replaced after 3 days.

GlcNAc and Kifunensine treatment of NSPCs:

A stock solution of 800 mM N-acetylglucosamine (GlcNAc, Fisher Scientific) was prepared in proliferation medium. For dose response experiments, the stock solution was added to E12 NSPC cultures in proliferation medium to create final concentrations ranging from 20 to 80 mM GlcNAc and the same concentration of GlcNAc was maintained in the differentiation medium (Grigorian et al., 2007). The medium was re-supplemented with fresh GlcNAc every 24 hours since GlcNAc breaks down over time in aqueous solutions. For some experiments NSPCs were treated with 80 mM GlcNAc for 3 days in proliferation medium then dissociated for analysis. Experiments designed to test the effects of GlcNAc at different stages of cell growth and differentiation used GlcNAc supplementation in either the proliferation medium only (and not the differentiation medium), the differentiation medium only (and not the proliferation medium), or treated throughout proliferation and differentiation so included in both media. When GlcNAc was added to differentiation medium, the GlcNAc stock was also prepared in differentiation medium and GlcNAc was re-supplemented daily in the culture media. Control cells were grown in medium lacking supplementation with GlcNAc. Kifunensine (0.5 µM, Sigma Aldrich) was added to proliferation medium in some experiments to block the incorporation of GlcNAc into highly branched N-glycans. Both kifunensine and GlcNAc were withdrawn during differentiation conditions in these experiments.

Proliferation Assays

Proliferation assays utilized phospho-histone H3 immunostaining or EdU incorporation as previously described (Lu et al., 2012). Cells undergoing mitosis were visualized by immunocytochemistry utilizing the primary antibody mouse anti-phospho-histone H3 (Ser10) (6G3) IgG (Cell Signaling Technology 9706S) and the secondary antibody donkey anti-mouse IgG Alexa Fluor 488 (Thermo Fisher Scientific A21202). All cells were counterstained with Hoechst 33342 nuclear dye (Thermo Fisher Scientific). Cells that passed through at least one S-phase were visualized using EdU incorporation (Click-iT EdU Alexa Fluor 555 Imaging Kit, Thermo Fisher Scientific). Proliferation medium of adherent NSPCs was supplemented with 10 μM EdU and cells incubated at 37^{o} C for 4 hours. Afterwards, cells were fixed and permeabilized as described above. After washing with PBS, cells were incubated with the EdU Click-iT reaction cocktail for 30 min at room temperature in the dark and counterstained with Hoechst 33342 nuclear dye (Thermo Fisher Scientific). Cells were analyzed using manual counting software in ImageJ and positively labeled cells were counted as a percentage of all Hoechst-stained cells in 5 randomly selected fields.

Cell Viability

Cell viability was assessed using the LIVE/DEAD Viability/Cytotoxicity Kit (for mammalian cells) (Thermo Fisher Scientific). Briefly, dissociated E12 NSPCs were re-suspended in 1 mL proliferation medium containing 100 nM calcein-AM to label live cells and 8 μM ethidium homodimer-1 to label dead cells. The cell suspension was incubated for 15-20 min at room temperature, protected from the light. Cell apoptosis was analyzed using the Dead Cell Apoptosis Kit (Thermo Fisher Scientific). Briefly, dissociated E12 NSPCs were re-suspended in the provided 5x Annexin V reaction buffer (50 mM HEPES, 700 mM NaCl, 12.5 mM $CaCl_2$, pH 7.4) containing Alexa Fluor 488-conjugated Annexin V and 1 μg/ml propidium iodide. The cell suspension was incubated for 10 min on ice, protected from the light. Control apoptotic cells were generated by culturing NSPCs at 37ºC in growth medium containing 200 μM H_2O_2 for 3 hours prior to analysis. The cells were analyzed with a BD LSR II flow cytometer, and the data collected using the BD FACSDIVA software. All data analysis was performed using FlowJo v10.1.

Immunocytochemistry and fate potential analysis

After differentiation, adherent cells were fixed with 4% paraformaldehyde (4% paraformaldehyde, 5 mM $MgCl_2$, 10 mM EGTA, 4% sucrose in PBS) for 10 min, and the cell membranes were permeabilized with 0.3% Triton-X 100 in PBS for 5 min. Cells were blocked using 5% BSA in PBS for 1 hour then incubated with the primary antibody for approximately 18 hours at 4^{o} C and the secondary antibody for 2 hours at room temperature in the dark. All cells were counterstained using a Hoechst 33342 nuclear dye (Thermo Fisher Scientific) and coverslips were mounted onto glass slides using VectaShield mounting medium (Vector Labs). Cells were visualized using a Nikon Eclipse Ti-E fluorescence microscope at 20x magnification, and all images were acquired using NIS Elements AR 4.51 image capturing and analysis software. Antibodies for immunostaining included mouse anti-MAP2 IgG (Sigma M9942) at 1:200, goat anti-DCX (C-18) IgG (Santa Cruz Biotechnology SC8066) at 1:200, rabbit-anti TUJ1 IgG (Sigma T2200) at 1:100, mouse anti-O4 IgM (R&D Systems MAB1326) at 1:100, or mouse anti-GFAP IgG (Sigma G9269) at 1:200 with all antibodies prepared in 1% BSA in PBS. Secondary antibodies donkey anti-mouse IgG Alexa Fluor 555, donkey anti-goat IgG Alexa Fluor 555, donkey-anti rabbit IgG Alexa Fluor 555, donkey anti-mouse IgG Alexa Fluor 488, and goat anti-mouse IgM heavy chain Alexa Fluor 555 (Thermo Fisher Scientific A31570, A21432, A21206, A21202, A21426) were diluted 1:200 in 1% BSA.

For fate analysis, at least 3 independent sets of NSPCs derived from 3 different litters were analyzed using manual counting software built into ImageJ. The percentage of cells that differentiated into double-positive MAP2/DCX or MAP2/TUJ1 neurons with neurite lengths of at least 3 times the length of the soma was calculated from 5 randomly selected fields per experiment with more than 1000 cells counted per experimental group in each of the 3 independent experiments, so over 3000 cells per group. The percentages of GFAP-positive astrocytes were calculated from randomly selected fields of cells adjacent to the sphere attachment site but not from the dense cells within the sphere since cell density and cell death affect astrocyte GFAP reactivity. Cells expressing GFAP in a filamentous cytoskeletal pattern were counted as astrocytes and 3000 or more cells per experimental group were analyzed.

RNA isolation, array, and qRT-PCR analysis

NSPC or E12 cerebral cortex total RNA was isolated using the Aurum total RNA isolation kit (Bio-Rad Laboratories), and cDNA was synthesized using M-MLV reverse transcriptase (Promega) in the S100 Thermal

Cycler (Bio-Rad) after which the enzyme was heat inactivated at 95^{o}C for 5 min. cDNA generated from E12 and E16 NSPC total RNA was analyzed using the RT^{2} Profiler PCR Array (Qiagen) for 84 glycosylation-related genes in mouse. Function of glycosylation enzymes is listed in Tables S1, S2, S3(Varki, 2009).

Analysis of glycosylation enzyme expression was performed using TaqMan probe-based gene expression assays with the Taqman universal PCR master mix (Life Technologies 4304437) and commercially available Taqman high specificity probes. Taqman probes used for qRT-PCR analysis included mouse actin (Mm00607939_s1), *18s* (Mm0392899_g1), *Man2a1* (Mm00484781_m1), *Man2a2* (Mm00556618_m1), *Mgat1* (Mm01288784_m1), *Mgat5* (Mm01291751_m1), *Fut8* (Mm00489789_m1), *St6gal1* (Mm00486119_m1), *St8sia2* (Mm0131039_m1), *St8sia4* (Mm01292231_m1) all from Life Technologies. In experiments analyzing astrocyte progenitor marker expression, qRT-PCR was performed using short oligonucleotide DNA primers customized through NCBI's Primer-BLAST (ordered from IDT) (see Table S4) and PowerUp™ SYBR® Green Master Mix (Thermo Fisher Scientific). All qRT-PCR experiments were performed using the ABI Viia7 instrument, and data was exported from the ABI Viia7 software. Data from the PCR arrayTaqman, and SYBR green assays were analyzed by the comparative cycle (C_t) method (Cheng et al., 2006). The PCR array C_t experimental data was normalized to internal array controls. The Taqman assay data utilized 18s or actin to normalize the experimental C_t values. The SYBR green assay used *Gapdh* as the reference gene. Where indicated, gene expression was further normalized to RNA isolated from whole E12 cerebral cortex or *in vitro* NSPC samples as indicated

RNA sequencing and analysis

RNA was isolated from suspended E12 mouse NSPC cultures from three separate litters using the Bio-Rad RNA Isolation Kit (Genicity, Irvine, CA, USA; G00065). Genomic DNA contamination of all RNA samples was assessed by using qRT-PCR for mouse 18S and *Gapdh* with and without reverse transcriptase and found to be insignificant. cDNA for qRT-PCR was synthesized using M-MLV reverse transcriptase (Promega). Total RNA was further monitored for quality control using the Agilent Bioanalyzer Nano RNA chip and Nanodrop absorbance ratios for 260/280nm and 260/230nm.

RNA library preparation and sequencing was performed at the UCI Genomics Core as previously described (Arulmoli et al., 2016). Library construction was performed according to the Illumina TruSeq mRNA stranded protocol. The input quantity for total RNA was 250ng and mRNA was enriched using oligo dT magnetic beads. The enriched mRNA was chemically fragmented for five minutes. First strand synthesis used random primers and reverse transcriptase to make cDNA. After second strand synthesis the double-stranded cDNA was cleaned using AMPure XP beads and the cDNA was end repaired and the 3' ends were adenylated. Illumina barcoded adapters were ligated on the ends and the adapter ligated fragments were enriched by nine cycles of PCR. The resulting libraries were validated by qPCR and sized by Agilent Bioanalyzer DNA high sensitivity chip. The concentrations for the libraries were normalized and the libraries were multiplexed together. The concentration for clustering on the flowcell was 12.5 pM. The multiplexed libraries were sequenced on one lane using single read 100 cycles chemistry for the HiSeq 2500. The version of HiSeq control software was HCS 2.2.58 with real time analysis software, RTA 1.18.64.

For sequence mapping and bioinformatic analysis, RNA-Seq data was processed as described previously (Lissner et al., 2015). All bioinformatics analyses were conducted using the Galaxy platform (Goecks et al., 2010). Reads were aligned to the mouse NCBI37/mm9 reference genome with the TopHat program (Trapnell et al., 2010) using most default parameters. Alignments were restricted to uniquely mapping reads with two possible mismatches permitted. RPKM (reads per kilobase pair per million mapped reads) were calculated as described (Mortazavi et al., 2008) for mm9 RefSeq genes using the SeqMonk program (http://www.bioinformatics.babraham.ac.uk/projects/seqmonk/). mRNA RPKMs were derived by counting exonic reads and dividing by mRNA length.

Membrane preparation and MALDI-TOF Mass Spectroscopy

Approximately 7x10^{7} NSPCs were washed with PBS containing 0.6% glucose twice. Cells were suspended in an ice-chilled hypotonic solution (1x PBS diluted 1:10) containing AEBSF and leupeptin protease inhibitors and lysed by freeze-thaw cycling between a dry ice/ethanol bath and 37^{o}C water bath. The sample was centrifuged at 75 x g for 15 min at 4^{o}C to remove nuclei, large organelles, and unlysed cells. The supernatant was collected and further centrifuged at 100,000 x g for 1 hour at 4^{o}C using a Beckman Ultracentrifuge (rotor TL110). The pellet containing the cell membrane fraction was isolated and sent to the Glycotechnology Core Facility of the Glycobiology Research and Training Center at the University of California, San Diego where MALDI-TOF Mass Spectroscopy

was performed as described by Lee *et al*. (Lee et al., 2007). Glycan species were obtained from E12 and E16 NSPCs and the total intensity measured for each glycan structure was analyzed. N-glycan species formed by core branching glycosylation enzymes were grouped according to the number of branches emanating from the core structure (1 to 4) and each group compared between E12 and E16 NSPCs. N-glycan species containing sialic acid or fucose residues were grouped to compare sialic acid or fucose containing N-glycans between E12 and E16 NSPCs.

Flow cytometry

Live E12, E16, GlcNAc-treated E12 NSPCs, or DEP sorted cells from E12 NSPCs were dissociated using NeuroCult and washed 3 times with 5% BSA in PBS. For labeling with lectins, 300,000 cells were re-suspended in 20 µg/mL FITC-conjugated lectin *Phaseolus vulgaris* leukagglutinin (L-PHA), 20 µg/mL FITC-conjugated lectin *Lens culinaris* agglutinin (LCA), or 40 µg/mL FITC-conjugated *Sambuca nigra* lectin (SNA) (Vector Labs) in 1% BSA and incubated in the dark at 4^{o} C for 1 hour. After washing 3 times with 1x PBS, cells were re-suspended in PBS containing 3 µM propidium iodide, which was used to exclude non-viable cells for analysis. For antibody labeling, cells were re-suspended in 1% BSA with unconjugated-monoclonal antibody against PSA-NCAM (clone 2-2B, Millipore MAB5324) and incubated at 4^{o} C for 30 min. Following washes in 1% BSA, cells were incubated in the dark at 4^{o} C for 30 min with donkey-anti mouse IgM Alexa Fluor 594 (Jackson ImmunoResearch 715-585-140). Cells were additionally stained using the Zombie Green™ Fixable Viability Kit (BioLegend) to exclude non-viable cells in analysis. All cells were analyzed on a BD LSR II flow cytometer, and the data was collected using the BD FACSDIVA software. All data analysis was performed using FlowJo v10.1.

DEP-based sorting of NSPCs

Mouse NSPCs were dissociated prior to sorting by dielectrophoresis (DEP) with non-enzymatic NeuroCult as described above. Dissociated cells were resuspended in DEP buffer, an iso-osmotic solution consisting of 8.5% (w/v) sucrose, 0.3% (w/v) glucose, and adjusted to a final conductivity of 110 µS/cm via addition of RPMI-1640 medium (Flanagan et al., 2008; Lu et al., 2012). DEP buffer conductivity was measured with a conductivity meter (Thermo Orion, Beverly, MA). The final cell concentration was adjusted to $1x10^{6}$ cells/mL for all DEP experiments.

The DEP device used for sorting experiments was fabricated as previously described and appropriate sorting parameters were used so that DEP had no effect on NSPC survival, proliferation or differentiation potential (Lu et al., 2012; Simon et al., 2014). Prior to DEP sorting, the DEP multi-well device was sterilized by UV light for 30-45 minutes, followed by washing with 70% EtOH (v/v), mQ H_2O, 0.05% trypsin-EDTA (v/v), and DEP buffer in sequential order in a sterile biosafety cabinet. Dissociated cells resuspended in DEP buffer were added to each well ($60x10^{5}$ cells per well) followed by a 10 minute incubation to ensure settling of all cells to the bottom of the wells. This was done to make sure the majority of cells were in close proximity to the electrodes. Cells were sorted by applying an AC electric field using a function generator AFG320 (Tektronix, Beaverton, OR) with 3 $V_{peak\text{-}peak}$ at 100 kHz (sorting frequency) for 5 minutes while 3 washes with DEP buffer removed cells not attracted to the electrodes. Control samples include cells exposed to 1 MHz (control frequency) for 5 minutes, since this frequency exposes cells to DEP but does not sort the cells, or cells incubated in DEP buffer without application of the electric field. Cells from these two controls did not differ in any of the analyses. Cells were collected and either processed for RNA analysis or flow cytometry as described above or plated in proliferation medium in 4mm diameter PDMS microwells on glass coverslips coated with pDL/laminin (Nourse et al., 2014). After 24 hours, the medium on the plated cells was switched to differentiation medium and cells were differentiated for 5 days prior to immunocytochemistry with anti-GFAP as described above.

DEP-based capacitance and cell size measurements

NSPCs were dissociated and suspended in DEP buffer as described above. DEP-based membrane capacitance measurements were obtained using the DEP-Well system, as described previously (Hoettges et al., 2008; Labeed et al., 2011). The DEP-Well was observed using a Nikon inverted microscope equipped with a 1.3 Mpixel video camera, and the change in light intensity across the well over time was determined using a MATLAB (The Mathworks Inc, Natick, MA) script. The well was energized with frequencies ranging from 1 kHz–20 MHz at 5 points per decade. Using MATLAB, light intensity measurements were fit to the single shell model (Broche et al., 2005) and the best-fit model (minimum line correlation coefficient 0.98) was used to determine the specific membrane capacitance (Cspec). Cell diameters were measured using ImageJ to analyze phase contrast microscopy images of trypan blue excluding cells in a hemocytometer.

Brain tissue section analysis:

Developing CD-1 mice embryos were collected at embryonic days E10, E12, E16, and E18. The whole embryo was collected for E10 embryos, the head for E12 embryos, and the brain dissected out at E16 and E18. Tissue was placed in 4% paraformaldehyde (PFA) for approximately 18 hours at 4°C then transferred to 30% sucrose in PBS until the tissue was no longer floating. For some antibodies (SOX1, SOX2), tissue was fixed in 4% PFA, 2% saponin for 2 hours at 4°C. Tissue was quickly frozen in Optimal Cutting Temperature (OCT) compound (Tissue-Tek) and stored at -80°C prior to sectioning. Cryosections (20 µm) were taken along the sagittal plane using a Leica research cryostat (Leica CM3050 S) and mounted on SuperFrost glass slides. Sections were washed with PBS and blocked for 20 min at room temperature with 3% BSA in PBS for lectin histochemistry or 5% donkey serum in PBS for antibody staining, with both solutions containing 0.1% Triton-X 100. For lectin staining, sections were incubated with diluted lectin in blocking solution for 1 hour at room temperature in a humidified chamber. For antibody staining, sections were incubated with primary antibody in blocking solution for 18 hours at 4°C in a humidified chamber then with secondary antibody for 1 hour at room temperature. All sections were counterstained with Hoechst 33342 nuclear dye (Thermo Fisher Scientific) and mounted using VectaShield (Vector Labs). Lectins included FITC-conjugated lectin *Phaseolus vulgaris* leukagglutinin (L-PHA) at 20 µg/mL (Vector Labs). Primary antibodies included goat anti-SOX1 IgG (Santa Cruz Biotechnology SC17318) at 1:50, goat anti-SOX2 IgG (Santa Cruz Biotechnology SC17320) at 1:200, goat-anti DCX (C-18) IgG (Santa Cruz Biotechnology SC8066) at 1:200, mouse anti-MAP2 IgG (Sigma M9942) at 1:200. Secondary antibodies included donkey anti-mouse Alexa Fluor 555 and donkey anti-goat Alexa Fluor 555 (Thermo Fisher Scientific A31570 and A21432) at 1:500. Images of the developing dorsal forebrain surrounding the lateral ventricle were taken using a Nikon Eclipse Ti-E fluorescent microscope at 20x magnification and the NIS image capturing software. The cortical plate (CP) and ventricular zone/subventricular zone (VZ/SVZ) were distinguished by MAP2/DCX for neurons in the CP and SOX1/SOX2 staining for NSPCs in the VZ/SVZ. A measuring box generated in ImageJ was used to quantify the average signal intensity in 10 randomly selected areas within each of the given regions and lectin-stained blood vessels were excluded from analysis. Maximum and minimum intensity values were recorded for each analyzed box and the minimum value was subtracted from the maximum to control for variations in staining intensity across different staining batches. One brain from a litter represented one biological repeat and at least 3 brains were analyzed for each embryonic stage.

Supplemental References

GeneCards: The Human Gene Database. In: Weizmann Institute of Science.

Arulmoli J, Wright HJ, Phan DT, Sheth U, Que RA, Botten GA, Keating M, Botvinick EL, Pathak MM, Zarembinski TI, Yanni DS, Razorenova OV, Hughes CC, Flanagan LA (2016) Combination scaffolds of salmon fibrin, hyaluronic acid, and laminin for human neural stem cell and vascular tissue engineering. Acta Biomater *43*,122-138.

Broche L, Labeed F, Hughes M (2005) Extraction of dielectric properties of multiple populations from dielectrophoretic collection spectrum data. Physics in Medicine and Biology *50*,2267-2274.

Cheng X, Hsu CM, Currle DS, Hu JS, Barkovich AJ, Monuki ES (2006) Central roles of the roof plate in telencephalic development and holoprosencephaly. J Neurosci *26*,7640-7649.

Flanagan LA, Lu J, Wang L, Marchenko SA, Jeon NL, Lee AP, Monuki ES (2008) Unique dielectric properties distinguish stem cells and their differentiated progeny. Stem Cells *26*,656-665.

Goecks J, Nekrutenko A, Taylor J, Team G (2010) Galaxy: a comprehensive approach for supporting accessible, reproducible, and transparent computational research in the life sciences. Genome Biol *11*,R86.

Grigorian A, Lee SU, Tian W, Chen IJ, Gao G, Mendelsohn R, Dennis JW, Demetriou M (2007) Control of T Cell-mediated autoimmunity by metabolite flux to N-glycan biosynthesis. J Biol Chem *282*,20027-20035.

Hoettges KF, Hübner Y, Broche LM, Ogin SL, Kass GE, Hughes MP (2008) Dielectrophoresis-activated multiwell plate for label-free high-throughput drug assessment. Anal Chem *80*,2063-2068.

Labeed FH, Lu J, Mulhall HJ, Marchenko SA, Hoettges KF, Estrada LC, Lee AP, Hughes MP, Flanagan LA (2011) Biophysical characteristics reveal neural stem cell differentiation potential. PLoS One *6*,e25458.

Lee SU, Grigorian A, Pawling J, Chen IJ, Gao G, Mozaffar T, McKerlie C, Demetriou M (2007) N-glycan processing deficiency promotes spontaneous inflammatory demyelination and neurodegeneration. J Biol Chem *282*,33725-33734.

Lissner MM, Thomas BJ, Wee K, Tong AJ, Kollmann TR, Smale ST (2015) Age-Related Gene Expression Differences in Monocytes from Human Neonates, Young Adults, and Older Adults. PLoS One *10*,e0132061.

Lu J, Barrios CA, Dickson AR, Nourse JL, Lee AP, Flanagan LA (2012) Advancing practical usage of microtechnology: a study of the functional consequences of dielectrophoresis on neural stem cells. Integr Biol *4*,1223-1236.

Mortazavi A, Williams BA, McCue K, Schaeffer L, Wold B (2008) Mapping and quantifying mammalian transcriptomes by RNA-Seq. Nat Methods *5*,621-628.

Nourse JL, Prieto JL, Dickson AR, Lu J, Pathak MM, Tombola F, Demetriou M, Lee AP, Flanagan LA (2014) Membrane biophysics define neuron and astrocyte progenitors in the neural lineage. Stem Cells *32*,706-716.

Simon MG, Li Y, Arulmoli J, McDonnell LP, Akil A, Nourse JL, Lee AP, Flanagan LA (2014) Increasing label-free stem cell sorting capacity to reach transplantation-scale throughput. Biomicrofluidics *8*,064106.

Trapnell C, Williams BA, Pertea G, Mortazavi A, Kwan G, van Baren MJ, Salzberg SL, Wold BJ, Pachter L (2010) Transcript assembly and quantification by RNA-Seq reveals unannotated transcripts and isoform switching during cell differentiation. Nat Biotechnol *28*,511-515.

Varki A (2009) Essentials of Glycobiology, 2 Edition. Cold Spring Harbor, New York: Cold Spring Harbor Laboratory Press.